Haghaei H., et al., *BioImpacts*, 2020, 10(1), 17-25
doi: 10.15171/bi.2020.03
http://bi.tbzmed.ac.ir/

Kinetic and thermodynamic study of beta-Boswellic acid interaction with Tau protein investigated by surface plasmon resonance and molecular modeling methods

Hossein Haghaei[1], Seyed Rafie Aref Hosseini[1], Somaieh Soltani[2], Farzaneh Fathi[3], Farzad Mokhtari[4], Saeed Karima[4], Mohammad-Reza Rashidi[2,3*]

[1] Nutrition and Food Sciences Faculty, Tabriz University of Medical Sciences, Tabriz, Iran
[2] Pharmacy Faculty, Tabriz University of Medical Sciences, Tabriz, Iran
[3] Research Center for Pharmaceutical Nanotechnology, Tabriz University of Medical Sciences, Tabriz, Iran
[4] Institute of Biochemistry and Biophysics, University of Tehran, Tehran, Iran

Article Info

Article Type:
Original Article

Article History:
Received: 21 Jan. 2019
Revised: 16 Apr. 2019
Accepted: 17 Apr. 2019
ePublished: 22 May 2019

Keywords:
Beta Boswellic acid
Tau protein
Kinetic study
Surface plasmon resonance

Abstract

Introduction: Beta-Boswellic acid (BBA) is a pentacyclic terpene which has been obtained from frankincense and its beneficial effects on neurodegenerative disorders such as Alzheimer's disease (AD) have been addressed.

Methods: In the present study, thermodynamic and kinetic aspects of BBA interaction with Tau protein as one of the important proteins involved in AD in the absence and presence of glucose has been investigated using surface plasmon resonance (SPR) method. Tau protein was immobilized onto the carboxy methyl dextran chip and its binding interactions with BBA were studied at physiological pH at various temperatures. Glucose interference with these interactions was also investigated.

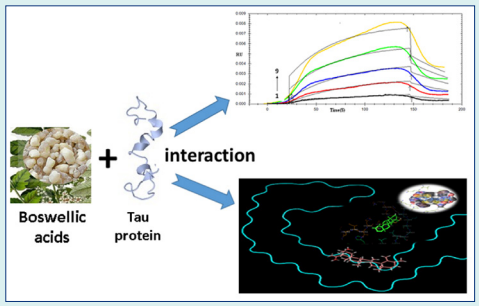

Results: Results showed that BBA forms a stable complex with Tau (K_D=8.45×10^{-7} M) at 298 K. Molecular modeling analysis showed a hydrophobic interaction between BBA and HVPGGG segment of R_2 and R_4 repeated domains of Tau.

Conclusion: The binding affinity increased by temperature enhancement, while it decreased significantly in the presence of glucose. Both association and dissociation of the BBA-Tau complex were accompanied with an entropic activation barrier; however, positive enthalpy and entropy changes revealed that hydrophobic bonding is the main force involved in the interaction.

Introduction

Neurodegenerative diseases (NDDs) are traditionally defined as disorders with selective and progressive loss of structure or function of neurons. Alzheimer's disease (AD) is one of the most common types of NDDs which is characterized by the progressive loss of memory and other cognitive functions.[1] Cognitive failure in the AD is the result of different co-pathologic interactions.[2] Different studies have suggested a central role for proteins in the development of AD. Accumulation of senile plaques leading to extracellular β-amyloid (Aβ) and intracellular neurofibrillary tangles (NFTs; pathologically aggregated Tau) are among the major hallmarks in the brain of the AD patients.[3] Attempts to find protein-based biomarkers for diagnostic aims and development of various therapeutic strategies were the results of improved understanding of protein role in AD.[4] In this regard, the development of vaccines against Tau protein has been explored.[5]

As an intrinsically disordered protein (IDP), Tau protein possesses a random coil (in solution) structure in physiologic conditions;[3] while in the AD, their aggregation leads to PHF-insoluble Tau (mostly β-sheet structure) (Fig. 1A-C).[6] This aggregation is a result of various physiologic factors such as oxidative stress and imbalance actions of kinases and phosphatases.[5,7,8]

Investigation of small molecules with the ability of

*Corresponding author: Mohammad-Reza Rashidi, Email: rashidi@tbzmed.ac.ir

binding to Tau protein or Tau physiologic function-related enzymes/drug targets have emerged as an interesting field in AD research[9]. Among these are natural compounds. Herbal remedies and food-derived agents as nutraceuticals have become more popular in the treatment of NDDs and the benefits derived from these phytotherapeutics have been very promising.[10]

Frankincense referred to as Oleo-gum resin which is extracted from the trees of the genus Boswellia of Burseraceae family and is obtained after an incision into the bark of the tree.[11] Beta-Boswellic acid (BBA) (Fig. 1D) is the most abundant compound in the extract of resins.[12] Yassin et al[13] reported the protective and therapeutic effects of Boswellia Serrata extract on the AD in rats (a decrease in the levels of NFTs in the affected regions of the brain). Additionally, in an in vitro study, it was shown that BBA is able to enhance neurite outgrowth, branching, and polymerization dynamics of tubulin.[14]

In the present study, the binding interaction of BBA with Tau protein and its kinetic and thermodynamic parameters were investigated using surface plasmon resonance (SPR) technique. The interaction was also studied in the presence of different concentrations of glucose. Glucose is the main source of energy for the brain.[15] Glucose deprivation can occur in aging and NDDs.[16] Clinical investigations have highlighted a biological link between reduced brain glucose metabolism and AD.[17] Diabetes and insulin resistance are strong risk factors for cognitive decline and AD.[18,19] The effect of glucose on tau aggregation both via interfering in Tau phosphorylation,[20] Tau cleavage and Tau glycation[17,21] have been considered as probable mechanisms in crosstalk between AD and diabetes.[21]

In addition, the effect of BBA on Tau stability and the secondary structure was studied by the application of CD measurements. Moreover, details of the interaction mechanism were investigated by the application of molecular docking and protein mapping studies. To the best of our knowledge, no similar study has been reported.

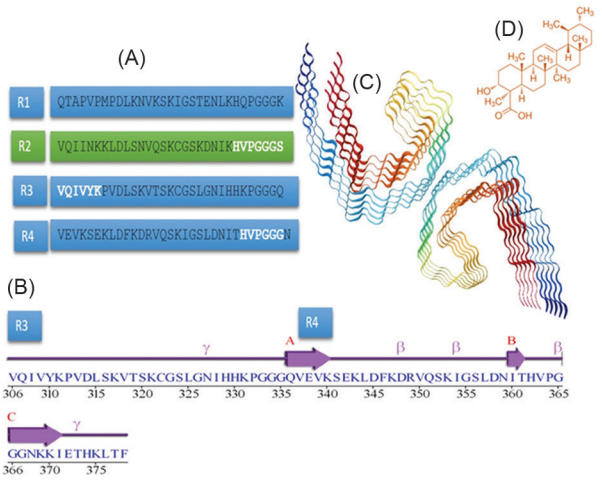

Fig. 1. (A) Amino acid sequence of R_1–R_4 of Tau repeat domains (microtubule-binding domains), (B) A sequence alignment of R_3 and R_4 repeat domains, (C) Schematic illustration of Tau protein paired filaments, (D) Chemical structures of Beta Boswellic acid.

Materials and Methods

Materials

Tau protein solution (in phosphate Buffer 50 mM) was purchased from biochemistry faculty of Shahid Beheshti University of Tehran. Its purity was checked by the application of the SDS-PAGE method[22] and its concentration was measured by Bradford total protein assay method.[23] Tau aliquots were stored at -70°C until analysis. Before analysis, Tau was transferred to -20°C for 12 hours and then gently thawed at room temperature.

BBA (purity >95%) was purchased from Sigma-Aldrich (Germany). BBA stock solution (1×10^{-3} M) was prepared by dissolving the proper amount of it in HPLC grade methanol (Scharlau) and stored in dark glass at 4°C. The amount of methanol in all samples was <1%.

Sodium hydroxide (NaOH), N-hydroxysuccinimide (NHS), N-ethyl- N'-(3-diethylaminopropyl) carbodiimide (EDC), PBS (Phosphate-Buffered Saline) tablets and ethanolamine were purchased from Sigma-Aldrich (Germany). All these ingredients were of analytical grade. All solutions were diluted to the required volume with PBS buffer (pH 7.4), prepared from double-distilled water (prepared daily in Lab).

SPR measurements

A multi-parameter SPR device (MP-SPR Navi 210A, BioNavis Ltd, Tampere-region, Finland) equipped with a Kretschman prism configuration and a goniometer was used for SPR measurements. A peristaltic pump equipped with 100×10^{-6} L sampler loops was applied to inject the mobile phases (PBS, pH 7.4) with the flow rate of 30×10^{-6} L/min to dual flow channels. The experiments were carried out in fixed-angle mode. Sensor temperature varied between 298-310 K. A laser with a wavelength of 670 nm was used as a light source to excite the surface plasmon at the dielectric gold interface. The bulk effects were corrected by subtracting the response of a blank reference spot from the response of the ligand spots.[24] Different concentrations of BBA ($1\text{-}9\times10^{-6}$ M) were injected with a flow rate of 30×10^{-6} L.min^{-1} for 2 minutes.

For minimizing the mass transport effect which leads to inaccurate data, the following approach was conducted in this study. First, the Tau molecule was immobilized using a low concentration Tau solution and the flow rate of test solutions for both kinetic and thermodynamic tests was set at a higher rate, i.e. 30×10^{-6} L.min^{-1}.

Carboxymethyl dextran (CMD) chips (Bionavis company, Finland) were used to immobilize Tau protein. These sensor chips were designed to allow detailed quantitative studies of small organic molecules, proteins interaction kinetics, and affinity. The ligands (Tau) were bounded to the sensor chip surface via carboxyl moieties on the dextran.

To obtain a stable baseline, PBS buffer (pH 7.4) was run

for 20 minutes onto the CMD chip. Then NaCl (1 M) and NaOH (0.1 M) was run for 5 minutes to both channels in order to sensor surface cleaning.

Tau immobilization was carried out using carbodiimide (amine coupling) strategy. The carboxylated surface of the cleaned chip was activated using a solution of EDC (0.2 M): NHS (0.05 M) (50/50 V/V) which was injected for 6 minutes and then rinsed with PBS buffer solution (pH 7.4) for 5 minutes. The surface activated slides were exposed to Tau solution (0.25 $mg.mL^{-1}$ with a flow rate of 8.0×10^{-6} $L.min^{-1}$ for 10 minutes). The non-specific bindings were prevented by the injection of ethanolamine-HCl (1.0 M) to the chip after Tau immobilization.[25]

Various concentrations of BBA (1-9×10^{-6} M) in PBS buffer (pH 7.4) were injected onto the Tau immobilized CMD chip (Tau-CMD) for 2 minutes. To investigate the nonspecific binding of BBA to the applied chip, a blank chip (without immobilized Tau) was inserted in the reference flow cell.

Investigation of glucose effect on BBA-Tau binding

To investigate the glucose effect in BBA-Tau interaction, Tau-CMD was inserted in both flow cells. BBA was injected into one of the chips after running a fixed flow rate of glucose on both chips. Various concentrations of BBA (1-9×10^{-6} M) in PBS buffer (pH 7.4) in the absence and presence of three separate concentrations (2.5, 5.0, and 20 $\times10^{-3}$ M) of glucose were injected for 2 minutes.

Study of Tau conformation after complex formation

To study the conformational variation of Tau due to BBA interaction, circular dichroism (CD) spectroscopy was used. CD spectra of Tau protein solution (20×10^{-6} M) before and after the addition of BBA (5.0×10^{-6} M) was recorded using a Jasco J-810 CD spectrometer (Lakewood, NJ, USA) equipped with a 0.1 cm path length sample cell. Data were collected with an interval of 1 nm (scan speed of 20 nm/min at298 K) in the wavelength range of 200-250 nm. The baseline was corrected according to the PBS buffer solution (pH 7.4). The average of two measurements was analyzed using CDNN 2.1 CD curve de-convolution software. This software uses a neural network approach for calculating secondary structure features of proteins.

Molecular modeling study of BBA-Tau interaction

Probable binding sites were investigated using an online small molecule protein mapping server FTMap. BBA was used as a probe ligand for a hairpin structure of Tau repeat domain. The suggested binding site along with a known aggregation driver motif of the R_3 domain (^{306}VQIVYK^{311})[26] was further investigated using molecular docking studies. BBA was docked to the selected motifs of Tau tubulin-binding repeat region crystal structure (PDB code: 5O3L, https://www.rcsb.org/structure/5O3L) using the gold software. The applied crystal structure was obtained using cryo-electron microscopy method[27] from the paired helical filament in the AD brain (Fig. 1C). We used chain A as a representative of suitable conformation for aggregation. Both protein and BBA structures were optimized prior to docking with MOE software.[28] A standard docking procedure was used to find suitable conformations. Accordingly, Goldscore scoring function analysis followed by a rescoring using ChemScore scoring function method was used for molecular docking studies. The results were viewed using LigandScout (http://www.inteligand.com/ligandscout/) and Pymol software and the best conformation was selected based on the frequency and orientation of the BBA in the studied binding site, while docking score was used for final selection between best results.

Results

Tau immobilization

Tau adsorption onto the activated surface of the chip could be achieved through both covalent amide coupling and electrostatic bond formation. Below the isoelectric pH of Tau (8.96), the amino groups possess positive charges,[25] while in this pH, carboxylic groups of CMD have negative charges. Therefore, the electrostatic bond formation is possible which facilitates the Tau attachment to the CMD chip surface at pH 7.4.

When a new layer was formed on Au sensor chip (e.g. CMD), the resonance curves shifted to higher incident angles and became wider which is a result of the increase in the thickness of the adsorbed layer. Accordingly, it is possible to evaluate the immobilization process through monitoring the response unit (RU) before and after Tau immobilization.

RU of untreated CMD was 0.01 which increased significantly to 0.025 after surface activation with EDC/NHS and decreased to 0.01 following surface cleaning. After the immobilization of Tau on the chip surface, RU value increased to 0.05. The remaining activated carboxylic acid groups were deactivated using ethanolamine (Fig. 2A). The steepest slope in the sensorgram occurred during the binding of Tau to the chip surface. This steep falling slope was consequent with a shift in total internal reflection (TIR).[29] The angle shift of CMD chip surface in comparison with the Tau-CMD chip has been shown in Fig. 2B. The angel shifted from 0.079 to 0.102 after Tau immobilization. According to the results of the activation of CMD, Tau immobilization was performed properly.

BBA-Tau interaction studies

The real-time binding profiles of BBA (1-9×10^{-6} M) with Tau have been presented in Fig. 3A. At all BBA concentrations, the responses reached equilibrium. The RU increased due to the BBA concentration enhancement.

K_D, K_a, and K_d values were obtained from fitting the equilibrium RU to a one-site binding model using Trace Drawer TM software. Kinetic properties of the binding procedure were produced using the SPR sensorgrams of

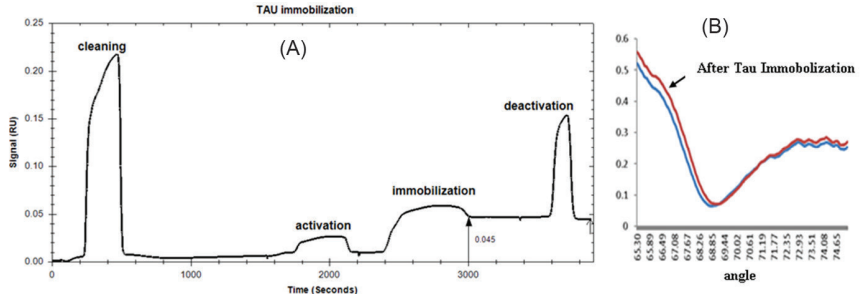

Fig. 2. (A) SPR sensogram of Tau immobilization on a CMD chip at PH 7.4 [Activation: activation of the CMD with a mixture of EDC/NHS (injection time: 6 min, flow rate: 30×10^{-6} L/min)- Immobilization: immobilization of 0.25 mg/mL Tau (injection time: 10 min, flow rate: 8×10^{-6} L/min)- Deactivation: deactivation of remaining reactive NHS esters with ethanolamine (injection time: 3 min, flow rate: 30×10^{-6} L/min)].

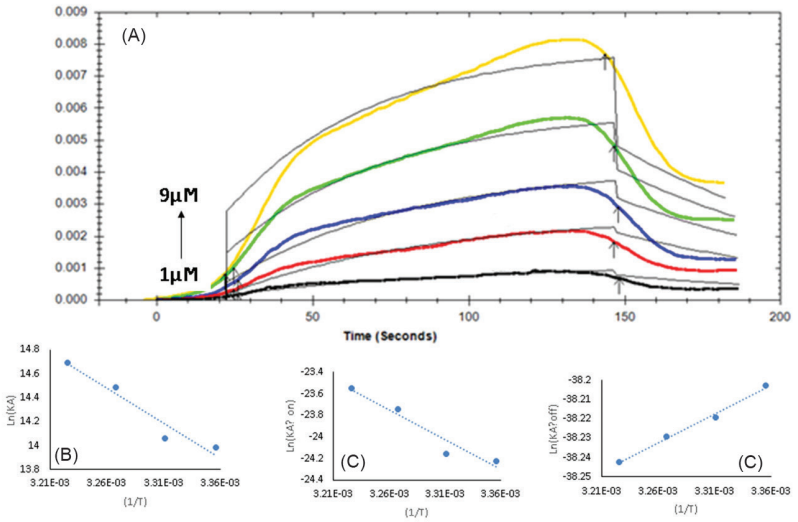

Fig. 3. (A) Sensogram BBA interaction with immobilized Tau (BBA 1-9×10^{-6} M), (B) Van't Hoff plot for binding of BBA to the Tau protein in temperature range from 298 to 310 K. (C) and (D) Eyring plot of association and dissociation rate constants of BBA-Tau interaction, respectively.

various BBA concentrations as a function of time.[30]

The value of K_D at 298 K was 8.45×10^{-6} M which shows the high affinity of BBA to Tau.[31] Furthermore, K_a and K_d values were calculated as 1.18×10^{3} $M^{-1}S^{-1}$ and 1.0×10^{-3} S^{-1}, respectively (Table 1). These results indicate that the rate constants have almost similar contribution in the binding of BBA molecules to Tau at 298 K.

Temperature dependence of the kinetics and affinity of the BBA interaction with Tau were investigated at various temperatures. The kinetic parameters were determined following injecting serially diluted concentrations of BBA in running buffer ($1\text{-}9\times10^{-6}$ M) to the Tau-CMD at various temperatures (298-310 K), and K_a, K_d and K_D values at different temperatures were calculated. The results are summarized in Table 1.

The results of fitting curves evaluated based on the theoretical one to one fitting model showed that RU values increase following increasing the BBA concentration (Fig. 3A). When these experiments were carried out at higher temperatures, it was found that the enhancement effect of BBA on RU values occurs at lower levels.

The K_D values decreased from 8.45×10^{-7}M at 298 K to 4.18×10^{-7}M at 310 K, suggesting that stronger bindings occur between Tau and BBA at higher temperatures. The association rate constant increased by 2.1 folds due to temperature enhancement from 298 K to 310 K, while the dissociation rate constant remained unchanged. This was well reflected in the corresponding K_D values. Therefore, the observed changes in the K_D values can be described by the increase in the association rate constant rather than a decrease in the dissociation rate constants.

Investigation of thermodynamic properties of BBA-Tau interaction

Van't Hoff plot (equation 1) was used to investigate the relationship between K_A and temperature.

Table 1. Kinetic data of BBA interaction with Tau

T (K)	K_d(1/S)×10^{-3}	K_a(1/ MS)×10^{3}	K_D(M)×10^{-7}
298	1.00	1.18	8.45
302	0.99	1.28	7.81
306	1.00	1.95	5.13
310	1.00	2.40	4.18

$$\ln(K_A) = -\left(\frac{AH^\circ}{RT}\right) + \left(\frac{AS^\circ}{R}\right) \quad \text{Eq. (1)}$$

where ΔH° and ΔS° are standard enthalpy and entropy changes respectively, R is gas constant and T is the absolute temperature.[32]

The standard ΔG° was calculated using the Gibbs free energy relationship (equation 2):

$$\Delta G^\circ = \Delta H^\circ - T\Delta S^\circ \quad \text{Eq. (2)}$$

Binding enthalpy (ΔH), entropy (ΔS) and Gibbs energy change (ΔG) along with K_A values of the interaction were calculated using the binding constants at different temperatures (Table 2).

The results showed that there is a linear relationship between K_A and 1/T (Fig. 3B). This result indicates that ΔH° and ΔS° were practically independent of temperature in the studied temperature range. The negative slope indicates that the studied binding reaction was endothermic and an increase in the temperature results in a subsequent increase in K_A value.

Calculated ΔG°, ΔH°, and ΔS° values at 298 K were -3.46×104, 4.86×104 Kcal/M and 2.79×102 Kcal/KM, respectively (Table 2).

The positive value of ΔH° indicates that the complex formation is an endothermic process and the standard enthalpy change upon the Tau-BBA complex formation is unfavorable. On the other hand, the positive ΔS° value indicates that entropy increases as the Tau-BBA complex is formed.

Negative ΔG° indicates that the binding reaction was thermodynamically favorable and proceeded spontaneously. It appears that the entropy and not the enthalpy drives the formation of the Tau-BBA complex. The spontaneous binding process is being driven by the entropy changes.

The transition state kinetics was studied using Eyring plot.[33] To obtain the activation of $\Delta H^{\circ\dagger}$ and $\Delta S^{\circ\dagger}$, Eyring equation (equation 3) was used.

$$\ln Kh/K_B T = \Delta H^{\circ\dagger}/RT + \Delta S^{\circ\dagger}/R \quad \text{(Eq. 3)}$$

where K is the rate constant for the activated complex determined at temperature T (the absolute temperature) in terms of $\Delta H^{\circ\dagger}$ and $\Delta S^{\circ\dagger}$, K_B is the Boltzmann constant (1.38×10^{-23}), and h is the Planck constant (1.05×10^{-34}). Therefore, by measuring the rate constants ($K=K_a$ or K_d) at different temperatures, it is possible to obtain $\Delta H^{\circ\dagger}$ and $\Delta S^{\circ\dagger}$ values for the assembly of Tau-BBA (Fig. 3C and 3D).

The formation of the transition state for binding of BBA to Tau was characterized by an unfavorable enthalpy and entropy; whereas, the dissociation phase proceeded with a favorable enthalpy and unfavorable entropy. A positive value for $\Delta H^\dagger$ in the association phase indicates that an unfavorable activation enthalpy (an activation enthalpy barrier) hinders the formation of the Tau-BBA transition state complex. On the other hand, there was a decrease in the enthalpic barrier to the transition state, facilitating the release of BBA from the Tau-BBA complex. Therefore, it seems that both association and dissociation of BBA and Tau are accompanied with an entropic activation barrier; however, the dissociation transition state of the complex is slightly compromised by a favorable enthalpy change in terms of the complex dissociation leading to the instability of the Tau-BBA complex.

Effects of glucose on Tau-BBA binding

BBA affinity to Tau was investigated in the presence of different concentrations of glucose. It was found that the presence of glucose interfered with the Tau-BBA complex formation in a way that affinity decreased significantly by the enhancement of glucose concentration (Table 3).

Conformational investigations

Fig. 4 shows far-UV CD spectra of Tau in the absence and presence of BBA. The double negative band around 208 (π →π*) and 222 nm (n→π*) and a positive band around 193 nm (π→π*) is characteristic for the typical α-helical structure for a pure α-helical structure,[34, 35] while a negative band around 196 nm reveals random coil in the protein structure.

The mentioned features can be seen in Fig. 4, for not treated Tau protein in the studied condition in which both alpha-helix and random coil determinant bands are available. A similar CD curve for Tau protein was reported in previous studies. The complex formation between Tau and BBA leads to a variation in the Tau protein CD curve comparing with its unbound form in which one positive band around 193 appears which shows that the BBA

Table 2. Thermodynamic parameters for binding of the BBA to the Tau protein in PBS buffer pH 7.4

	Vant's Hoff			Eyring Plot (K_a)			Eyring Plot (K_d)		
T (K)	ΔH (Kcal/M) ×10⁴	ΔS (Kcal/KM) ×10²	ΔG° ×10⁴	ΔH (Kcal/M) ×10⁴	ΔS (Kcal/KM) ×10	ΔG° ×10⁴	ΔH (Kcal/M)×10³	ΔS (Kcal/KM) ×10²	ΔG° ×10⁴
298	4.86	2.79	-3.46	4.65	-4.63	6.03	-2.48	-3.27	9.48
302			-3.57			6.05			9.61
306			-3.68			6.07			9.74
310			-3.79			6.08			9.87

Table 3. Kinetic data of BBA-Tau interaction in the presence of glucose

Glucose (mM)	k_d(1/S)×10^{-4}	k_a(1/ MS)×10^{3}	K_D(M)×10^{-7}
0	9.92*	2.2*	4.51*
2.5	9.96	1.89	5.26
5.0	9.86	1.39	7.10
20	9.98	1.24	8.02

*Derived from experiments in which reference cell consists of CMD-Tau.

binding leads to an increase in the α-helical structure of the Tau protein.[36]

The calculated percentage of random coil and β-sheet in unbound Tau solution was 42.0% and 27.9%, respectively. After BBA (5×10^{-6} M) addition, the random coil and β-sheet was 40.7% and 24.9%, respectively. The α-helical content of Tau increased from 12.5% to 16.7% after BBA addition, which could be an indicator of the stability enhancement of Tau after complex formation with BBA.[37] It seems that BBA induces certain perturbations (increasing α-helical structure) on the Tau protein secondary structure which could affect the physiologic function of Tau.

Molecular modeling of the Tau–BBA interaction

Protein mapping revealed that there is a conserved hexapeptide in the R_4 domain of studied Tau filament (^{362}HVPGGG^{367}) (Fig. 1A), which possessed a probability of interaction with BBA (Fig. 5). In addition, the literature review shows that (^{306}VQIVYK^{311}) hexapeptide (R_3) is one of the most important motifs which is playing role in Tau aggregation.[38, 39] We investigated the molecular interaction of BBA with both hexapeptides using molecular docking studies. The results showed that the interaction pattern for the studied sites is different. These findings suggest that BBA can be situated near the (^{362}HVPGGG^{367}) segment with a higher probability (ΔG=-21.24 kcal.mol^{-1} for the best score) (Fig. 5) in comparison to (^{306}VQIVYK^{311}) (ΔG=-17.46 kcal.mol^{-1} for the best score) considering the best scores, and the average ΔG for all conformations are -17.05 kcal.mol^{-1} and -15.19 kcal.mol^{-1}, respectively for (^{306}VQIVYK^{311}) and (^{362}HVPGGG^{367}).

The molecular docking results showed that hydrophobic interactions are the main driving force for the binding which is consistent with the experimental results.

Discussion

As a widely used optical method for ligand interaction analysis, the SPR approach can be used for real-time monitoring of the small molecule-target affinity.[40] The association and/or dissociation of the studied analyte to the immobilized protein leads to changes in mass transfer and subsequently influence the refractive index at the surface layer.[41] Variation in the refractive index causes changes in the SPR signal (RU). It is possible to determine both association and dissociation rate constants (k_a and k_d) separately. The equilibrium dissociation constant (binding affinity), K_D, can be calculated from the ratio of k_d to k_a for a given interaction. The k_a constant can be regarded as the number of BBA-Tau complex formed per second and the k_d is the fraction of the complex decays per second.[42] according to the results the enhanced binding of BBA to Tau at higher temperatures could arise from a better diffusion of BBA molecules and its increased collision to the immobilized Tau at higher temperatures.

Previous evidence has identified that the positive ΔH° and ΔS° values are normally considered as the evidence for the hydrophobic interaction[32, 43]; it could be assumed that the binding of BBA to Tau occurs mainly through hydrophobic interactions. Additionally, the positive values

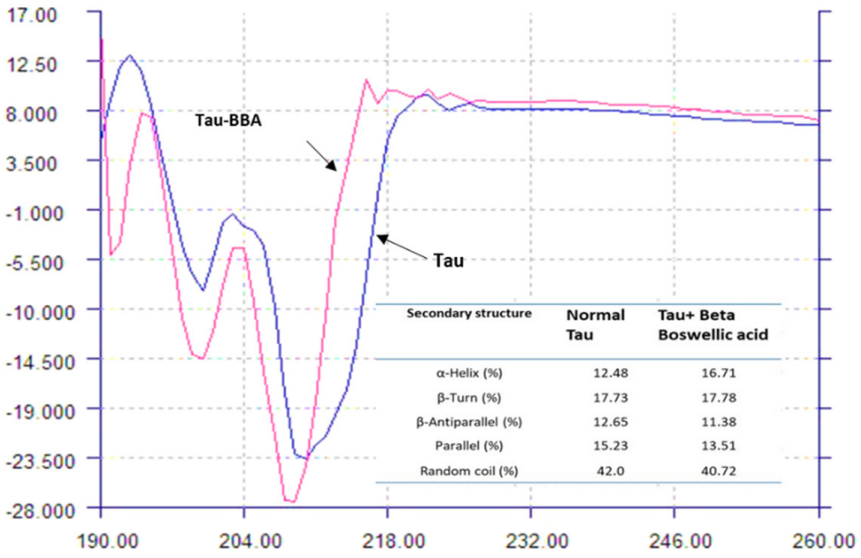

Figure 4. CD spectra of Tau in the absence and presence of BBA (190-260 nm). Tau = 20×10^{-6}M, BBA = 0-5.0×10^{-6} M.

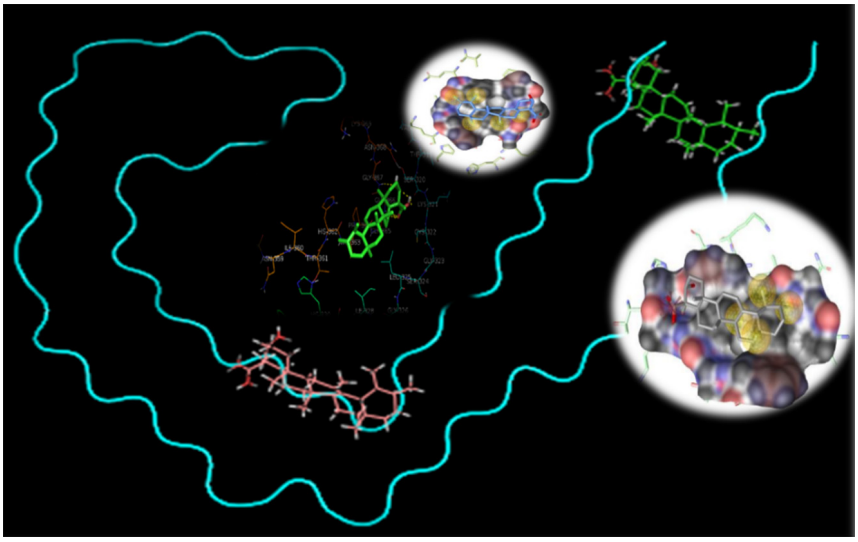

Figure 5. Molecular docking and protein mapping results of Tau–BBA interaction (PDB ID 5OL3).

of ΔH°, and ΔS° and the negative value of ΔG° indicate that the overall thermodynamic stability of Tau-BBA complex comes from an entropy/enthalpy balance. Accordingly, a favorable TΔS° term outweighs the unfavorable ΔH°, and the hydrophobic interactions play a major role in the binding of BBA to Tau.

According to the previous studies,[21] there are different glycation sites on Tau protein; therefore, it is expected to be a common interaction site for BBA and glucose on Tau protein, and the competition between BBA and glucose for interacting with these binding sites can cause the decreased affinity by the increase of glucose concentration. But these underlying mechanisms of the current results are subject to further investigation.

It is well-known that β structures are needed for the aggregation of disordered proteins and studies showed that Tau aggregation is driven by a transition from random coil to β- sheet structure.[44] while different studies suggested that α-helix could be a driver of primary accumulation and aggregation for disordered proteins.[45] It seems that BBA induces certain perturbations (increasing α-helical structure) on the Tau protein secondary structure which could affect the physiologic function of Tau.

From the above data, (^{362}HVPGGG^{367}) segment can be found both in R_2 and R_4 domains. It could be assumed that BBA can interact with both R_2 and R_4 domains, while protein mapping suggested no interaction with a similar segment (i.e. ^{330}HKPGGG^{335}) in R_3. The (PGGG) conserved segments in R_1-R_4 are responsible for making (PGGG) loops, which have a role in stabilizing microtubules after assembly making.[46] It is obvious both from SPR studies and molecular docking results that BBA interacts with different repeat domains of Tau, while the crystal structure of Tau is not available.[47] Therefore, the precise sites of repeat domains of Tau that is involved in the interaction with BBA should be further studied.

Conclusion

We reported the application of SPR and molecular modeling methods for the investigation of BBA interaction with Tau protein. The developed real-time and label-free method was able to determine both kinetic and thermodynamic properties of the interaction readily and accurately.

Results showed that BBA forms a stable complex with Tau (K_D=8.45×10^{-7} M) at 298 K. The binding affinity increased by temperature enhancement. The Tau-BBA complex formation decreased significantly in the presence of glucose. It may indicate that there is a common interaction site between BBA and glucose on Tau protein and BBA competes with glucose to interact with these binding sites. Kinetic analysis revealed that both association and dissociation of BBA and Tau are accompanied by an entropic activation barrier; however, the dissociation transition state of the complex is slightly compromised by a favorable enthalpy change. Positive enthalpy and entropy changes revealed that hydrophobic interactions are the main force of interaction between BBA and Tau. These results were in agreement with molecular modeling analysis which showed that BBA can be situated near the (^{362}HVPGGG^{367}) segment of R_2 and R_4 repeated domains of Tau through hydrophobic interactions.

The probable effect of BBA on Tau aggregation and also interfering of glucose with the binding of BBA to Tau molecule could be further investigated via in vitro studies. Taking into account the potential therapeutic uses of BBA in neurodegenerative disorders such as AD, the developed method would allow researchers to gain a better understanding of the mechanism of action of BBA and also other food-derived compounds in these diseases.

Acknowledgment

The authors acknowledge the partial financial support of the current study by Tabriz University of Medical Sciences under grant number of

D/P/3 which was a part of the Ph.D. thesis of Dr. Hossein Haghaei.

Funding Sources
Tabriz University of Medical Sciences under grant number of D/P/3.

Ethical statement
The authors declare no ethical issue to be considered.

Competing interests
The authors declare no conflicts of interest.

Authors' contribution
MRR, SRAH, HH: conceptualization and writing & reviewing; MRR, HH; data handling; FF, HH: experiments design; SS, HH: data analysis; SK, FM, HH: provision of study materials and equipment; SS,HH: study validation; MRR, SRAH: supervision; MRR, HH: data presentation, draft preparation and project administration; SK, FM, HH: study consultation;

Research Highlights

What is the current knowledge?
√ BBA interferes with AD path-ways.
√ BBA binds to the microtubules.
√ Tau protein aggregation is one of the pathological hallmarks of AD.
√ Hyperglycemia relates to Diabetes and AD.

What is new here?
√ Hydrophobic interactions are the main force of BBA-Tau interaction.
√ BBA binds to the Tau protein.
√ BBA situates near the (^{362}HVPGGG^{367}) segment of R2 and R4 which are important for Tau aggregation.
√ The binding affinity of BBA to Tau decreases significant-ly in the presence of Glucose.

References

1. Nieoullon A. Neurodegenerative diseases and neuroprotection: current views and prospects. *J Appl Biomed* **2011**; 9: 173–83. doi:10.2478/v10136-011-0013-4.
2. Huang Y, Mucke L. Alzheimer mechanisms and therapeutic strategies. *Cell* **2012**; 148: 1204-22. doi:10.1016/j.cell.2012.02.040.
3. Mandelkow E-M, Mandelkow E. Biochemistry and cell biology of tau protein in neurofibrillary degeneration. *Cold Spring Harb Perspect Med* **2012**; 2: a006247. doi:10.1101/cshperspect.a006247.
4. Halliday M, Mallucci GR. Targeting the unfolded protein response in neurodegeneration: a new approach to therapy. *Neuropharmacology* **2014**; 76: 169-74. doi:10.1016/j.neuropharm.2013.08.034
5. Wang Y, Mandelkow E. Tau in physiology and pathology. *Nat Rev Neurosci* **2016**; 17: 22. doi:10.1038/nrn.2015.1.
6. Von Bergen M, Barghorn S, Biernat J, Mandelkow E-M, Mandelkow E. Tau aggregation is driven by a transition from random coil to beta sheet structure. *Biochim Biophys Acta* **2005**; 1739: 158-66. doi:10.1016/j.bbadis.2004.09.010
7. Morris M, Maeda S, Vossel K, Mucke L. The many faces of tau. *Neuron* **2011**; 70: 410-26. doi:10.1016/j.neuron.2011.04.009.
8. Martin L, Latypova X, Wilson CM, Magnaudeix A, Perrin M-L, Terro F. Tau protein phosphatases in Alzheimer's disease: the leading role of PP2A. *Ageing Res Rev* **2013**; 12: 39-49. doi:10.1016/j.arr.2012.06.008.
9. Panza F, Seripa D, Solfrizzi V, Imbimbo BP, Santamato A, Lozupone M, et al. Tau aggregation inhibitors: the future of Alzheimer's pharmacotherapy? *Expert Opin Pharmacother* **2016**;17(4):457-61. doi: 10.1517/14656566.2016.1146686.
10. Williams P, Sorribas A, Howes M-JR. Natural products as a source of Alzheimer's drug leads. *Nat Prod Rep* **2011**; 28: 48-77. doi:10.1039/c0np00027b.
11. Zhang Y, Ning Z, Lu C, Zhao S, Wang J, Liu B, et al. Triterpenoid resinous metabolites from the genus Boswellia: pharmacological activities and potential species-identifying properties. *Chem Cent J* **2013**. doi: 10.1186/1752-153X-7-153.
12. Gerbeth K, Hüsch J, Fricker G, Werz O, Schubert-Zsilavecz M, Abdel-Tawab M. In vitro metabolism, permeation, and brain availability of six major boswellic acids from Boswellia serrata gum resins. *Fitoterapia* **2013**; 84: 99-106. doi:10.1016/j.fitote.2012.10.009
13. Yassin NAZ, El-Shenawy SMA, Mahdy KA, Gouda NAM, Marrie AEFH, Farrag ARH, et al. Effect of Boswellia serrata on Alzheimer's disease induced in rats. *J Arab Soc Med Res* **2013**; 8: 1–11. doi: 10.7123/01.JASMR.0000429323.25743.cc.
14. Karima O, Riazi G, Yousefi R, Movahedi AAM. The enhancement effect of beta-boswellic acid on hippocampal neurites outgrowth and branching (an in vitro study). *Neurol Sci* **2010**; 31: 315-20. doi:10.1007/s10072-010-0220-x.
15. De Felice FG, Lourenco MV. Brain metabolic stress and neuroinflammation at the basis of cognitive impairment in Alzheimer's disease. *Front Aging Neurosci* **2015**; 7: 94. doi:10.3389/fnagi.2015.00094
16. Castellano C-A, Nugent S, Paquet N, Tremblay S, Bocti C, Lacombe G, et al. Lower brain 18F-fluorodeoxyglucose uptake but normal 11C-acetoacetate metabolism in mild Alzheimer's disease dementia. *J Alzheimers Dis* **2015**; 43: 1343-53. doi: 10.3233/JAD-141074
17. Lauretti E, Li J, Di Meco A, Pratico D. Glucose deficit triggers tau pathology and synaptic dysfunction in a tauopathy mouse model. *Transl Psychiatry* **2017**; 7: e1020. doi: 10.1038/tp.2016.296
18. Morris JK, Honea RA, Vidoni ED, Swerdlow RH, Burns JM. Is Alzheimer's disease a systemic disease? *Biochim Biophys Acta* **2014**; 1842: 1340-9. doi:10.1016/j.bbadis.2014.04.012
19. Schubert M, Gautam D, Surjo D, Ueki K, Baudler S, Schubert D, et al. Role for neuronal insulin resistance in neurodegenerative diseases. *Proc Natl Acad Sci U S A* **2004**; 101: 3100-5. doi:10.1073/pnas.0308724101
20. Lauretti E, Pratico D. Glucose deprivation increases tau phosphorylation via P 38 mitogen-activated protein kinase. *Aging Cell* **2015**; 14: 1067-74. doi:10.1111/acel.12381
21. Liu K, Liu Y, Li L, Qin P, Iqbal J, Deng Y, et al. Glycation alter the process of tau phosphorylation to change tau isoforms aggregation property. *Biochim Biophys Acta* **2016**; 1862: 192-201. doi:10.1016/j.bbadis.2015.12.002
22. Dunn MJ. editore. *Gel electrophoresis of proteins*, Elsevier; **1986**. doi:10.1016/C2013-0-06476-6
23. Kruger NJ. The Bradford Method for Protein Quantitation. In: Walker JM, ed. *Basic Protein and Peptide Protocols. Methods in Molecular Biology™*. vol 32. Humana Press; 1994. p.9-15. doi:10.1385/0-89603-268-X:9
24. Etayash H, Jiang K, Azmi S, Thundat T, Kaur K. Real-time detection of breast cancer cells using peptide-functionalized microcantilever arrays. *Sci Rep* **2015**; 5: 13967. doi: 10.1038/srep13967
25. Fathi F, Dolatanbadi JEN, Rashidi M-R, Omidi Y. Kinetic studies of bovine serum albumin interaction with PG and TBHQ using surface plasmon resonance. *Int J Biol Macromol* **2016**; 91: 1045-50. doi: 10.1016/j.ijbiomac.2016.06.054
26. Seidler P, Boyer D, Rodriguez J, Sawaya M, Cascio D, Murray K, et al. Structure-based inhibitors of tau aggregation. *Nat Chem* **2018**; 10 (2): 170-176. doi: 10.1038/nchem.2889.
27. Fitzpatrick AW, Falcon B, He S, Murzin AG, Murshudov G, Garringer HJ, et al. Cryo-EM structures of tau filaments from Alzheimer's disease. *Nature* **2017**; 547(7662):185-190. doi: 10.1038/nature23002.
28. Poureshghi F, Ghandforoushan P, Safarnejad A, Soltani S. Interaction of an antiepileptic drug, lamotrigine with human serum albumin (HSA): Application of spectroscopic techniques and molecular modeling methods. *J Photochem Photobiol B* **2017**; 166: 187-92. doi:10.1016/j.jphotobiol.2016.09.046

29. Camero S, Benítez MJ, Cuadros R, Hernández F, Ávila J, Jiménez JS. Thermodynamics of the interaction between Alzheimer's disease related to tau protein and DNA. *PLoS One* **2014**; 9: e104690. doi:10.1371/journal.pone.0104690
30. Rispens T, Te Velthuis H, Hemker P, Speijer H, Hermens W, Aarden L. Label-free assessment of high-affinity antibody–antigen binding constants. Comparison of bioassay, SPR, and PEIA-ellipsometry. *J Immunol Methods* **2011**; 365: 50-7. doi:10.1016/j.jim.2010.11.010
31. Lundström I. Real-time biospecific interaction analysis. *Biosensors Bioelectron* **1994**; 9: 725-36. doi: 10.1016/0956-5663(94)80071-5
32. Sharifi M, Dolatabadi JEN, Fathi F, Rashidi M, Jafari B, Tajalli H, et al. Kinetic and thermodynamic study of bovine serum albumin interaction with rifampicin using surface plasmon resonance and molecular docking methods. *J Biomed Opt* **2017**; 22: 037002(1-6). doi:10.1117/1.JBO.22.3.037002
33. Li X, Song S, Shuai Q, Pei Y, Aastrup T, Pei Y, et al. Real-time and label-free analysis of binding thermodynamics of carbohydrate-protein interactions on unfixed cancer cell surfaces using a QCM biosensor. *Sci Rep* **2015**; 5: 14066. doi: 10.1038/srep14066
34. Greenfield N. Using circular dichroism spectra to estimate protein secondary structure. *Nat Protoc* **2006**; 1: 2876-2890. doi:10.1038/nprot.2006.202
35. Berger J, Dorninger F, Forss-Petter S, Kunze M. Peroxisomes in brain development and function. *Biochim Biophys Acta* **2016**; 1863: 934-55. doi:10.1016/j.bbamcr.2015.12.005
36. Jangholi A, Ashrafi-Kooshk MR, Arab SS, Riazi G, Mokhtari F, Poorebrahim M, et al. Appraisal of the role of the polyanionic inducer length on amyloid formation by 412-residue 1N4R Tau protein: a comparative study. *Arch Biochem Biophys* **2016**; 609: 1-19. doi:10.1016/j.abb.2016.09.004
37. Kelly SM, Jess TJ, Price NC. How to study proteins by circular dichroism. *Biochim Biophys Acta* **2005**; 1751: 119-39. doi:10.1016/j.bbapap.2005.06.005
38. Ait-Bouziad N, Lv G, Mahul-Mellier A-L, Xiao S, Zorludemir G, Eliezer D, et al. Discovery and characterization of stable and toxic Tau/phospholipid oligomeric complexes. *Nat Commun* **2017**; 8: 1678. doi:10.1038/s41467-017-01575-4
39. Mukrasch MD, Biernat J, von Bergen M, Griesinger C, Mandelkow E, Zweckstetter MJJoBC. Sites of tau important for aggregation populate β-structure and bind to microtubules and polyanions. *J Biol Chem* **2005;**280: 24978-24986. doi: 10.1074/jbc.M501565200
40. He J, Li S, Xu K, Tang B, Yang H, Wang Q, et al. Binding properties of the natural red dye carthamin with human serum albumin: Surface plasmon resonance, isothermal titration microcalorimetry, and molecular docking analysis. *Food Chem* **2017**; 221: 650-6. doi:10.1016/j.foodchem.2016.11.124.
41. Fabini E, Fiori GM, Tedesco D, Lopes NP, Bertucci C. Surface plasmon resonance and circular dichroism characterization of cucurbitacins binding to serum albumins for early pharmacokinetic profiling. *J Pharm Biomed Anal* **2016**; 122: 166-72. doi:10.1016/j.jpba.2016.01.051
42. Myszka DG. Kinetic analysis of macromolecular interactions using surface plasmon resonance biosensors. *Curr Opin Biotechnol* **1997**; 8: 50-7. doi:10.1016/S0958-1669(97)80157-7
43. Ross PD, Subramanian S. Thermodynamics of protein association reactions: forces contributing to stability. *Biochemistry* **1981**; 20: 3096-102. doi: 10.1021/bi00514a017
44. Hall GF. The biology and pathobiology of tau protein. *Cytoskeleton and Human Disease*: Springer; **2012**. p. 285-313. doi:10.1007/978-1-61779-788-0_15
45. Kim B, Do TD, Hayden EY, Teplow DB, Bowers MT, Shea J-E. Aggregation of Chameleon Peptides: Implications of α-Helicity in Fibril Formation. *J Phys Chem* **2016**; 120: 5874-83. doi:10.1021/acs.jpcb.6b00830
46. Kar S, Fan J, Smith MJ, Goedert M, Amos LA. Repeat motifs of tau bind to the insides of microtubules in the absence of taxol. *EMBO J* **2003**; 22: 70-7. doi:10.1093/emboj/cdg001
47. Jayapalan S, Natarajan J. The role of CDK5 and GSK3B kinases in hyperphosphorylation of microtubule associated protein tau (MAPT) in Alzheimer's disease. *Bioinformation* **2013**; 9: 1023-30. doi:10.6026/97320630091023